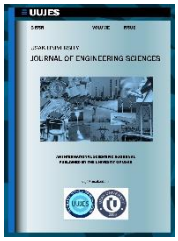

Usak University

Journal of Engineering Sciences

An international e-journal published by the University of Usak

Journal homepage: dergipark.gov.tr/uujes

Review article

QUANTUM RADAR: THEORY, LIMITS, and PRACTICAL APPLICATIONS

Murat Can Karakoç[1,2], Abdurrahman Can Kıraç[1], Özgün Ersoy[1], Asaf Behzat Şahin[1]*

[1]Department of Electrical and Electronics Engineering, Ankara Yıldırım Beyazıt University, Türkiye
[2]Department of Electrical and Electronics Engineering, Erzurum Technical University, Türkiye

Received: October 30, 2024 Revised: December 11, 2024 Accepted: December 26, 2024
Online available: December 30, 2024

Abstract

This paper provides a detailed exploration of quantum radar technology, focusing on the generation, measurement, and theoretical analysis of quantum-correlated signals in both optical and microwave domains. We examine the mechanisms behind producing entangled signals and their application to improve radar sensitivity and accuracy in noisy environments. A review of key studies is presented, with emphasis on their experimental setups and the limitations that define the potential of quantum radar. By aggregating data on object detection range and analyzing global research trends through visualizations, including a bar chart and a world map, we illustrate the growing interest and research efforts in this domain. Our findings highlight the significant advancements and remaining challenges in developing practical quantum radar systems, as well as the worldwide collaboration driving progress in this cutting-edge field.

Keywords: *Quantum radar; entanglement; two mode squeezed vacuum; Josephson junction; spontaneous parametric downconversion.*

List of Abbreviations Frequently Used in The Text

Abbreviation	Explanation
ADC	Analog-to-digital converter
APD	Avalanche photodiode
BBO	Beta-barium borate
BS	Beamsplitter
CCD	Charge-coupled device
CW	Continuous wave

*Corresponding author:
E-mail: muratcan.karakoc@aybu.edu.tr

DOI: 10.47137/uujes.1576274

DM	Dichroic mirror
DSF	Dispersion-shifted LEAF fiber
EDFA	Erbium-doped fiber amplifier
eJPA	Engineered Josephson parametric amplifier
EOM	Electro-opto-mechanical converter
JPA	Josephson parametric amplifier
JPC	Josephson parametric converter
JRM	Josephson ring modulator
JTWPA	Josephson traveling wave parametric amplifier
MgO:PPLN	Magnesium-oxide doped periodically-poled lithium niobate
PBS	Polarization beam splitter
ppKTP	Poled potassium titanyl phosphate
ROC	Receiver operating characteristics
SPAD	Single-photon avalanche diode
SPD	Single photon detector
SPDC	Spontaneous parametric downconversion
SNSPD	Superconducting single-photon detector
TMN	Two mode noise
TMSV	Two mode squeezed vacuum
QI	Quantum illumination
QTMS	Quantum two mode squeezing

1. Introduction

A seminal paper in [1] showed that quantum illumination which uses a quantum mechanical phenomenon known as entanglement enhances detectability of a target even in the lossy and noisy environment which destroys entanglement. Although the early work in [1] illustrated extremely important improvement on the detection of a target correctly, a couple of follow-up studies [2-3] showed that it is limited in terms of error probability exponent to the classical counterpart in theory.

Quantum radar was studied in the optical domain in [1-3], namely, the target was assumed to be illuminated with an optical source in those theoretical analyses. In this respect, experimental works in which the entangled source for illuminating the target in the optical domain has been conducted basically in [4-12]. In those experimental analysis, nonlinear crystal and semiconductor waveguides have been employed in order to generate entangled signal pairs. Meanwhile, detection schemes vary from single photon detectors to cameras in the optical domain.

After a study in [13] on microwave quantum illumination led to paradigm shift in the quantum radar concept and raised the interest of researchers on the quantum radar in the microwave domain, rather than optical domain. The microwave domain signal generation was carried out by employing an electro-opto-mechanical (EOM) converter in [13]. Superconducting circuits with Josephson junctions in an extremely low temperature were a good candidate for creating a couple of entangled signals. Therefore, Josephson parametric amplifier (JPA) was utilized in [14-18] instead of using the EOM converter to produce a pair of entangled signals in the microwave domain as in [13]. Depending on the JPA in [14] and the theoretical analysis in [2], the study in [15] approaches quantum radar from an engineering view, demonstrating that a quantum radar system can be derived from a classical noise radar by making specific assumptions in modelling. A similar study to [14], employing Josephson parametric converter (JPC) was also accomplished in [19] with an optimum receiver proposed at an early theoretical analysis on quantum radar at [20].

Performance of an engineered JPA (eJPA) proposed in [21] was compared to the quantum radar proposed in [16] and [19], separately. Rather than comparing the performance of the classical noise radar and the quantum radar as in the early studies, the impact of temperature and squeezing parameter on the purity and decoherence effects in the quantum radar observed in [22]. In addition, the research in [23] provides insights into the behaviour of entanglement, squeezing, and entropy in quantum radar, offering valuable implications for quantum information processing in the radar. Furthermore, in a quantum radar simulation, the improvement in performance between a non-degenerate JPA and a degenerate JPA through was examined in [24]. Rather than employing JPA/JPC in [14, 21], Josephson traveling wave parametric amplifier (JTWPA) was utilized [25-28].
The study in [29] evaluates the performance of microwave quantum radar, focusing on its maximum detection range and quantum advantage. Furthermore, advancing quantum radar technology into a broader area discussed in [30]. It is also important to note that potential medical sensing applications of microwave quantum radar were discussed in [31].

While several review articles on quantum radar have been published [32–39], they often lack a direct focus on the engineering perspective of microwave radar systems, despite contributions from authors with engineering backgrounds. This study bridges that gap by offering a comparative analysis of photon and signal generation techniques in the optical and microwave domains while also establishing a theoretical framework for measuring quantum information in both regimes. We examine the design and implementation of transmitter and receiver systems, highlight methodological differences in signal processing between optical and microwave quantum radars, and evaluate their operational ranges. Furthermore, we provide statistical insights into global interest in quantum radar, presenting data on research activity from Google Scholar to reflect contributions from various researchers and countries. By consolidating complex research into a more accessible format, this study aims to advance understanding, identify performance enhancement strategies, and provide guidance for future developments in quantum radar technology.

This paper, it is organized starting with a theoretical background on the generation of entangled pairs of signals in Section 2. Then, nonlinear materials to generation quantum correlated signal pairs for quantum radar is mentioned in Section 3, and measurement techniques in optical and microwave domain is detailed in Section 4. Following that, theoretical limits of quantum radar are indicated in Section 5. Practical applications and an analysis on quantum radar works are specified in Section 6 and Section 7, respectively. Finally, this paper is completed with conclusion and references in Section 8 and Section 9, consecutively.

2. Theoretical Background

The classical pump mode at frequency w_P interacts in a nonlinear medium with two modes at frequency w_S called signal frequency, and w_I called idler frequency, as shown in Fig. 1, where $w_P = w_S + w_I$. The Hamiltonian of a parametric amplifier system which generates highly correlated photon pairs is described as in Eq. (1).

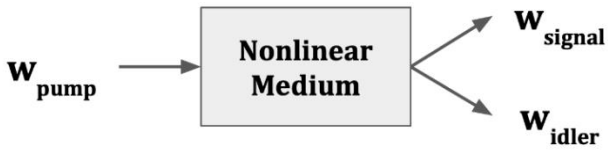

Fig. 1 Nonlinear interaction

$$H = \hbar w_S \hat{a}_S^\dagger \hat{a}_S + \hbar w_I \hat{a}_I^\dagger \hat{a}_I + j\hbar\Gamma\left(\hat{a}_S^\dagger \hat{a}_I^\dagger e^{-j2wt} - \hat{a}_S \hat{a}_I e^{-j2wt}\right) \quad (1)$$

where $\hat{a}_S^\dagger(\hat{a}_I^\dagger)$ and $\hat{a}_S(\hat{a}_I)$ are the annihilation and creation operators of the signal(idler) mode, $\hbar$ is a reduced Plank's constant, and Γ is the coupling parameter which is proportional to the amplitude of the pump (w_P) and the second-order susceptibility of the medium [40-42].

The equations of motion in the Heisenberg picture for the interaction representation are in Eq. (2),

$$\frac{d\hat{a}_S}{dt} = \Gamma \hat{a}_I^\dagger \quad (2.a)$$

$$\frac{d\hat{a}_I^\dagger}{dt} = \Gamma \hat{a}_S \quad (2.b)$$

The solutions to these equations can be expressed as Eq. (3),

$$\hat{a}_S = \hat{a}_S \cosh \Gamma t + \hat{a}_I^\dagger \sinh \Gamma t \quad (3.a)$$

$$\hat{a}_I = \hat{a}_I \cosh \Gamma t + \hat{a}_S^\dagger \sinh \Gamma t \quad (3.b)$$

The mean photon number in one mode after a time t for an initial coherent state, $|\alpha_S, \alpha_I\rangle$, is in Eq. (4),

$$\langle n_S(t)\rangle = \langle \alpha_S, \alpha_I | \hat{n}_S(t) | \alpha_S, \alpha_I \rangle \quad (4.a)$$

$$= \left\langle \alpha_S, \alpha_I \middle| \hat{a}_S^\dagger \hat{a}_S \middle| \alpha_S, \alpha_I \right\rangle \quad (4.b)$$

$$= |\alpha_S \cosh \Gamma t + \alpha_I^* \sinh \Gamma t|^2 + \sinh^2 \Gamma t \quad (4.c)$$

The number of photons generated when the system is started in the vacuum state ($\alpha_S = \alpha_I = 0$) is $\sinh^2 \Gamma t$ as in the last term in Eq. (4.c) [40, 43]. In a two mode system given as signal and idler is observed cross-correlations, which has a quantum behavior in intensity correlation functions. The two mode intensity correlation function is described as Eq. (5),

$$g_{SI}^{(2)}(0) = \frac{\left\langle \hat{a}_S^\dagger \hat{a}_S \hat{a}_I^\dagger \hat{a}_I \right\rangle}{\left\langle \hat{a}_S^\dagger \hat{a}_S \right\rangle \left\langle \hat{a}_I^\dagger \hat{a}_I \right\rangle} \quad (5)$$

When the signal and idler modes are symmetric, the appropriate Cauchy-Schwarz inequality is in Eq. (6),

$$\left[g_{SI}^{(2)}(0)\right]^2 \leq g_S^{(2)}(0) g_I^{(2)}(0) \quad (6.a)$$

$$\left\langle \hat{a}_S^\dagger \hat{a}_S \hat{a}_I^\dagger \hat{a}_I \right\rangle^2 \leq \left\langle \left(\hat{a}_S^\dagger \hat{a}_S\right)^2 \right\rangle \left\langle \left(\hat{a}_I^\dagger \hat{a}_I\right)^2 \right\rangle \quad (6.b)$$

$$\left\langle \hat{a}_S^\dagger \hat{a}_S \hat{a}_I^\dagger \hat{a}_I \right\rangle \leq \left\langle \left(\hat{a}_S^\dagger\right)^2 (\hat{a}_S)^2 \right\rangle + \left\langle \hat{a}_I^\dagger \hat{a}_I \right\rangle \quad (6.c)$$

$$g_{SI}^{(2)}(0) \leq g_S^{(2)}(0) + \frac{1}{\left\langle \hat{a}_I^\dagger \hat{a}_I \right\rangle} \quad (6.d)$$

The correlations that form reach the highest level permitted by the principles of quantum mechanics [40].

2.1. Two Mode Squeezed Vacuum (TMSV)

Quantum correlations developed between the signal and idler modes give rise to the squeezing observed in the non-degenerate parametric amplifier [40-44]. The total field according to the Heisenberg picture of the signal and idler mode where frequencies are placed symmetrically around w, as in Eq. (7).

$$E(t) = \frac{1}{\sqrt{2}}\left[\hat{a}_S(t)e^{-j(w+\varepsilon)t} + \hat{a}_S^{\dagger}(t)e^{j(w+\varepsilon)t} + \hat{a}_I(t)e^{-j(w+\varepsilon)t} + \hat{a}_I^{\dagger}(t)e^{j(w+\varepsilon)t}\right] \quad (7.a)$$

$$E(t) = X_\theta(t,\varepsilon)\cos(wt+\theta) - P_\theta(t,\varepsilon)\sin(wt+\theta) \quad (7.b)$$

where $\hat{a}_S$ and $\hat{a}_I$ were defined in Eq. (3) and the quadrature phase operators are defined in Eq. (8),

$$X_\theta(t,\varepsilon) = \frac{1}{2}\left[\left(\hat{a}_S(t)e^{j\theta} + \hat{a}_I^{\dagger}(t)e^{-j\theta}\right)e^{j\varepsilon\theta} + \left(\hat{a}_S^{\dagger}(t)e^{-j\theta} + \hat{a}_I(t)e^{j\theta}\right)e^{-j\varepsilon\theta}\right] \quad (8.a)$$

$$P_\theta(t,\varepsilon) = \frac{1}{2}\left[\left(\hat{a}_S(t)e^{j\theta} - \hat{a}_I^{\dagger}(t)e^{-j\theta}\right)e^{j\varepsilon\theta} + \left(\hat{a}_S^{\dagger}(t)e^{-j\theta} - \hat{a}_I(t)e^{j\theta}\right)e^{-j\varepsilon\theta}\right] \quad (8.b)$$

In the homodyne detection, where $\varepsilon = 0$ and $\theta = 0$, variances of the quadratures as in Eq. (9),

$$V\left(X_0(t,\varepsilon=0)\right) = e^{2\Gamma t} \quad (9.a)$$

$$V\left(P_0(t,\varepsilon=0)\right) = e^{-2\Gamma t} \quad (9.b)$$

2.2. TMSV and Entanglement

In order to measure the degree of correlation between the quadratures of the signal and idler modes, variance of the position quadratures (X_θ, X_ϕ) as in Eq. (10),

$$V(\theta,\phi) \equiv \frac{1}{2}\langle\left(X_S^{\theta}, X_I^{\phi}\right)^2\rangle \quad (10)$$

When $V(\theta,\phi) = 0$, then X_S^{θ} is perfectly correlated with X_I^{ϕ} [40]. This implies that measuring X_S^{θ} allows the clearly finding of X_I^{ϕ} [40].

The theoretical framework of the TMSV and entanglement, as outlined through the quadrature correlations and their variances, provides the foundation for its practical implementation in quantum radar systems. In essence, the squeezing observed in the non-degenerate parametric amplifier highlights the quantum correlations between the signal and idler modes, enabling the enhanced detection sensitivity that distinguish quantum radar from classical systems. The transition from this theoretical understanding to experimental setups involves careful consideration of how TMSV states are generated, manipulated, and measured in both the optical and microwave domains.

3. Generating Quantum Correlated Signals for Quantum Radar

Quantum radar represents a significant advancement in detection technology by exploiting quantum mechanical principles to enhance performance beyond classical limits. In particular, the use of quantum states, such as entanglement and squeezing, enables improved sensitivity, resolution, and resilience against noise, making it a promising tool in both optical and microwave frequency domains. In this section, it is explored the mechanisms for generating entangled and squeezed signals in both the optical and microwave domains.

3.1. Generating Signals in The Optical Domain

One of the most common methods for generating entangled photon pairs is through nonlinear optical processes like spontaneous parametric down-conversion (SPDC). In an SPDC process, a high-energy photon interacts with a nonlinear crystal, such as Beta-Barium Borate (BBO) or periodically-poled crystals like MgO and ppKTP, producing two lower-energy entangled photons. Similarly, semiconductor waveguides and birefringent

optical fibers are also employed in the generation of entangled signals by enabling precise control over photon properties like polarization and phase.

3.1.1. BBO Crystal

BBO Crystal is a nonlinear optical crystal commonly used in the generation of entangled photons through spontaneous parametric down-conversion (SPDC). BBO crystals exhibit high transparency over a wide wavelength range and are valued for their large nonlinear coefficients, making them suitable for various quantum optics experiments. They are often used in Type-I or Type-II phase matching configurations to produce polarization-entangled photon pairs [4, 5].

A pair of entangled signals is generated employing BBO crystal as shown in Fig. 2.a [4]. While one of the pairs illuminates the object with an additional noise, the other pair is transmitted directly to the camera. In order to observe the advantage of quantum radar compared to the classical counterpart, it is required that the target should be in a noisy environment [1]. Then both reflected signal from the object and the idler signal directly from BBO are measured at the camera.

3.1.2. Type-0 MgO:PPLN Crystal

Type-0 MgO:PPLN crystal is a nonlinear crystal used in quantum optics for the generation of entangled photon pairs. The periodic poling structure allows for quasi-phase matching, enabling efficient frequency conversion, such as second-harmonic generation or SPDC [45]. The doping with magnesium oxide increases the crystal's damage threshold, enhancing its robustness for high-power applications [46], [47]. Type-0 phase matching means that both down-converted photons share the same polarization [6].

Entangled photon pairs are generated with an SPDC process by utilizing a type-0 MgO:PPLN crystal as shown in Fig. 2.b [6]. The generated signal and idler photon pairs are spatially separated and directed into distinct optical paths using dichroic mirrors (DMs), which exploit their wavelength-selective reflection and transmission properties. The noisy background on the illuminated target is supplied by injection of additional noise via erbium-doped fiber amplifier (EDFA). The signal is combined with noise employing beam splitter as shown in Fig. 2.b. While the transmitted signal is reflecting from the object, idler signal is stored in a dispersion-shifted LEAF fiber (DSF).

3.1.3. ppKTP Crystal

ppKTB Crystal is an another type of nonlinear crystal frequently used for entangled photon generation via SPDC. Potassium titanyl phosphate (KTP) is periodically poled to achieve quasi-phase matching [48]. ppKTP is widely favored in quantum optics due to its high nonlinear coefficient and efficiency in generating entangled photons over a broad wavelength domain [49].

A system employing ppKTP crystal to find the range of a target is illustrated in Fig. 2.c [7]. In a continuous wave (CW) pumped ppKTP crystal, photon pairs are generated for range estimation purposes. One photon from the pair is retained locally, while the other is directed towards the target. By measuring the time difference between the two photons, the distance to the target can be determined. This is because the idler photon experiences a delay corresponding to the round-trip travel time to and from the target [7].

3.1.4. Birefringent Optical Fiber

Birefringent optical fiber is an optical fiber that exhibits different refractive indices for different polarization states of light [50]. Birefringent fibers can be used to manipulate the polarization of photons and are useful in maintaining entanglement by ensuring that polarization states remain distinct over long distances [50]. They play a critical role in preserving quantum coherence in fiber-based quantum communication systems.

Birefringent fiber cable is employed to generate a pair of entangled signals in [8] depending on the idea proposed by [50]. The power controlled pump signal is transmitted over a birefringent fiber cable and the produced entangled signal pairs are separated using dichroic beam splitter as shown in Fig. 2.d [8]. Then, while one of them is transmitted for illuminating the target, the other one is retained for handling in the measurement.

3.1.5. Semiconductor Waveguide

Semiconductor waveguide is a nanostructured medium used for guiding light, often fabricated from materials like silicon or gallium arsenide. Semiconductor waveguides are utilized in integrated photonic circuits for the generation and manipulation of entangled photons [51]. Due to their compact size and high efficiency, they enable scalable quantum photonic technologies and are essential for developing on-chip quantum optics systems [9-12].

The entangled pair of signals are generated by using semiconductor waveguides in a cryogenic environment in order to illuminate a target as illustrated in Fig. 2.e [11]. The generated signals are separated using polarization beam splitter (PBS). While one of them is transmitted for illuminating the target and the other one stored in the system [11]. After that, both reflected and retained photons are measured in order to detect the target.

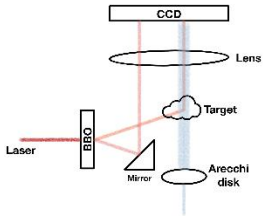

(a) BBO[4]

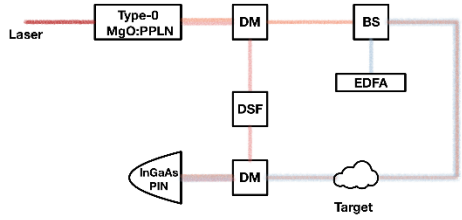

(b) MgO:PPLN(SPDC) [6]

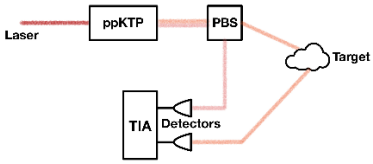

(c) ppKTP [7]

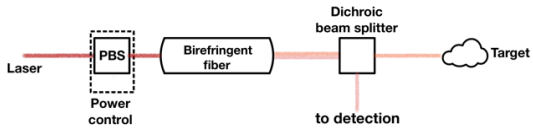

(d) Birefringent optical fiber [8]

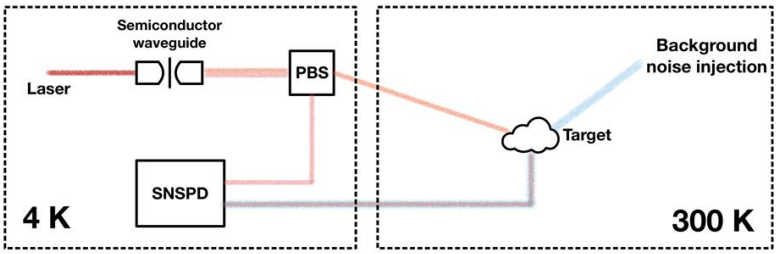

(e) Semiconductor waveguide [11]

Fig. 2 Optical domain quantum correlated signal generation and measurement setups

3.2. Generating Signals in The Microwave Domain

In the microwave regime, quantum illumination relies on the generation and manipulation of entangled or squeezed microwave signals using specialized quantum devices. Key components for generating these quantum signals include JPA [14], JPC [19], and JTWPA [25]. These superconducting devices leverage the nonlinear properties of Josephson junctions to produce squeezed and entangled microwave states that improve target detection sensitivity by reducing noise and increasing the signal-to-noise ratio.
The main distinction in generating entangled signal pairs in the microwave domain by employing JPA/JPC and JTWPA compared to the optical domain is that it requires extremely low cryogenic temperatures, around 10 mK. In these experiments, a 10 mK environment is essential to reduce thermal noise, maintain superconductivity, enhance parametric amplification, and preserve quantum coherence.

The picture and illustration of a dilution fridge where a 10 mK temperature can be achieved are shown in Fig. 3.a and Fig. 3.b respectively. JPA/JPC and JTWPA are placed at the bottom of the dilution fridge as shown in the Fig, 3.a, in which 10 mK can be reached. The produced signals are transferred from bottom to the top of the dilution fridge, then one of them is transmitted to the target and the other pair is directly measured by using a digitizer as shown on Fig. 3.b. After that the received signal reflected from the target and the idler signal which is measured directly are compared to controlling the existence of the target in an observation area.

3.2.1. JPA

The JPA generates entangled microwave signals by leveraging the nonlinear properties of Josephson junctions to amplify vacuum fluctuations, thereby producing squeezed states [52-55]. These squeezed states can exhibit reduced quantum noise in one quadrature, which, when combined with another signal, forms an entangled state. JPAs are critical in enhancing the signal-to-noise ratio for quantum illumination by creating entangled microwave modes useful for detection [14, 16].

Quantum radar using JPA to generate a pair of entangled signals, called quantum two mode squeezing (QTMS) radar, was studied in [16] to have much better performance in terms of receiver operating characteristics (ROC) compared to the classical noise radar, called two mode noise (TMN) radar. Moreover, the analyses depending on JPA performed in [16] were expanded to include effects on integration time and correlation coefficient in [17] and [18], respectively. Furthermore, eJPA has greater bandwidth and achieves more than 6 dB performance improvement in comparison to the classical counterpart [21].

3.2.2. JPC

The JPC operates similarly to a JPA but is designed to both amplify and convert signals between different frequencies. It generates entangled microwave states by mixing two or more frequency modes, producing correlations between the signal and idler modes. It can be designed as shown in Fig. 3.c known as a Josephson ring modulator (JRM) structure [19], [56]. This frequency conversion process ensures that the generated entangled signals can be optimized for quantum illumination in specific operational frequency domains [19].

3.2.3. JTWPA

The JTWPA extends the capabilities of JPAs by generating entangled signals over a broad bandwidth. Using a long array of Josephson junctions as shown in Fig 3.d, it enables continuous-wave parametric amplification, producing squeezed and entangled states across multiple frequency modes. This makes JTWPA particularly suitable for scalable quantum illumination applications requiring wide bandwidths and low noise over long distances [25, 28].

(a) JPA in dilution refrigerator [14] (test setup)

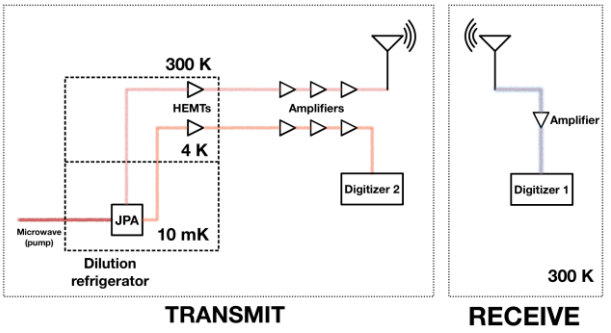

(b) JPA in dilution refrigerator [14] (illustration of test setup)

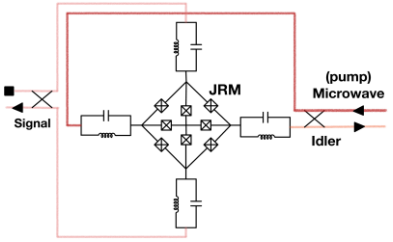

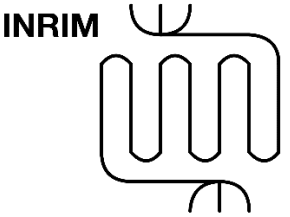

(c) Entangled signal generation in JPC [19] (d) Entangled signal generation in JTWPA [25]

Fig. 3 Microwave domain quantum correlated signal generation and measurement setups

4. Measuring Quantum Information for Quantum Radar

In quantum radar, quantum information refers to the entanglement shared between signal and idler photons, which enables the extraction of target information through their correlated states. The key advantage lies in using entanglement to enhance signal detection by correlating the idler photon, retained at the receiver, with the reflected signal photon. This process allows the system to distinguish the weak target signal from environmental

noise and interference, improving detection sensitivity and fidelity beyond what is achievable with classical radar techniques.

4.1. Measuring Quantum Information in The Optical Domain

In order to acquire quantum information about detecting a target in a given range, a CCD camera is employed for intensity correlation as shown in Fig. 2.a. This CCD camera captures spatially resolved data, enabling the analysis of photon distributions across specific correlated pixel pairs.

An SPAD camera is used to get both intensity and coincidence correlation information. Coincidence correlation of two photons has been inferred using the arriving time of the two quantum correlated photons [5]. Namely, a predefined time window is used to determine whether detection events at both detectors occur "simultaneously" (within the resolution of the setup). This ensures that the measured events correspond to correlated photons. The SPAD camera utilized in [5] is a special type of camera produced by using the SPAD array [57] which was already designed from the same research group, at which each pixel has time information about the arrival of photons both reflected and stored. In designing this type camera, achieving precise time gating with a resolution as fine as 5.75 ns and sub-40 ps gate shifts posed significant challenges in ensuring synchronization and timing accuracy across the large pixel array [57].

Moreover, single photon detectors (SPDs), i.e. InGaAs PIN detector [6], avalanche photodiode (APD) detector [7], [8], superconducting single-photon detector (SNSPD) [9-12] is used for detecting the target with the coincidence correlation. SPDs are highly sensitive devices capable of detecting individual photons by converting the energy of a single photon into an electrical signal, enabling precise measurements at the quantum level. APDs operate in Geiger mode, where APDs detect photons by amplifying a single electron-hole pair into a detectable current pulse. They are commonly used in quantum cryptography and time-correlated photon counting. SPADs are a specialized subset of APDs, SPADs offer high sensitivity and fast response times. They are widely used in imaging applications and quantum experiments due to their compact size and ability to integrate into arrays. SNSPDs achieve near-unity detection efficiency, extremely low dark count rates, and picosecond timing resolution. SNSPDs are made from superconducting materials placed in a cryogenic temperature, around 4 K shown in Fig 2.e.

4.2. Measuring Quantum Information in The Microwave Domain

Deducing quantum information from the signal reflected from the target and idler stored in the system requires the measurement to be done at the same time, otherwise it is not possible to get quantum advantage in coincidence correlation measurements. This is one of the disadvantages in the optical domain quantum radar systems. Even if it is required to cool down to cryogenic temperature for generating quantum correlated signals, around 10mK, reflected signal and idler photons are not needed at measurement at the same time in the microwave domain. Existence of a target has been detected with a couple of post-processing after measuring both signals. This post-processing depends on the covariance matrix analysis.

Both classical radar and quantum radar, the detection of the presence of the target is done by the analysis of the covariance matrix and the Pearson correlation coefficient [15]. The superiority of the quantum radar emerges at this point, in other words, the Pearson correlation coefficient is higher in quantum radar [2], [16]. The covariance matrix formed as a result of the measurement made in an environment where any target exists with very

low reflectance within the observation area and this target is exposed to high noise is as in Eq. (11),

$$\Lambda = \frac{1}{4}\begin{bmatrix} A & 0 & \sqrt{\kappa}C_{c/q} & 0 \\ 0 & A & 0 & -\sqrt{\kappa}C_{c/q} \\ \sqrt{\kappa}C_{c/q} & 0 & S & 0 \\ 0 & -\sqrt{\kappa}C_{c/q} & 0 & S \end{bmatrix} \tag{11}$$

where, these parameters are defined in Eq. (12),

$$C_C \equiv 2N_S \tag{12.a}$$
$$C_q \equiv 2\sqrt{N_S(N_S+1)} \tag{12.b}$$
$$A \equiv 2N_S + B \tag{12.c}$$
$$S \equiv 2N_I + 1 \tag{12.d}$$
$$B \equiv 2N_B + 1 \tag{12.e}$$

where C_C and C_q represent classical and quantum correlations, respectively. N_S, N_I, and N_B represent the transmitted, stored, and noise photon numbers, respectively. While κ represents the reflection coefficient of the target, A and B are used for the variation values of the transmitted and idler signals. All these observations, the Pearson correlation coefficient, ρ, is written as in Eq. (13) [15],

$$\kappa = \frac{\sqrt{\kappa}C_{c/q}}{\sqrt{A}\sqrt{S}} \tag{13}$$

In Eq. (13), the target can be detected with an analysis such that if ρ is above a certain value, the target is present, if it is below, the target is absent. The superiority of quantum radar emerges at this point. Since the C_q coefficient shows a higher correlation than C_c even when quantum entanglement disappears, it increases the probability of correctly detecting the target. Finally, although it is known that entanglement disappears during these measurements, it has been shown that it shows a higher correlation than the classical system thanks to the superiority provided by quantum physics.

4.2.1. Processing of Quantum Information in The Microwave Domain

While transferring quantum information into the classical world is provided by using detectors as mentioned in section 4.1 in the optical domain, in the microwave domain, digitization of quantum information is fundamentally provided by analog-to-digital converter (ADC) [16], [19]. The amplified and filtered signals are digitized using an ADC with a sampling rate depending on the commercial ADC product. This step converts the analog quadrature voltages of the signal and idler into digital data for further processing. The digitized data is the extracted quadrature voltages (I and Q) of the signal and idler modes. These voltages represent the real and imaginary parts of the electromagnetic field, essential for analysing quantum correlations [19]. The covariance matrix of the signal and idler states in (11) is reconstructed from the processed quadrature data. This matrix quantifies the quantum correlations and is used to evaluate the signal-to-noise ratio (SNR).

5. Comparison of The Optical and Microwave Quantum Radar Setups

Optical and microwave quantum radar systems differ significantly in their setups due to the fundamental differences between photons in the optical and microwave domains. Optical quantum radar setups typically involve the use of nonlinear crystals like periodically-poled lithium niobate (PPLN) or potassium titanyl phosphate (ppKTP) to

generate entangled photon pairs via spontaneous parametric down-conversion (SPDC). These systems are compact and capable of high-resolution imaging due to the shorter wavelengths of optical photons. However, they are more susceptible to losses caused by atmospheric scattering and absorption, making them less effective over long distances or in adverse weather conditions. Detection often involves single-photon detectors like avalanche photodiodes (APDs) or superconducting nanowire detectors (SNSPDs), which require precise alignment and cooling.

On the other hand, microwave quantum radar setups rely on superconducting devices like Josephson Parametric Amplifiers (JPAs) or Traveling Wave Parametric Amplifiers (JTWPAs) to generate and manipulate entangled microwave signals, such as two-mode squeezed vacuum (TMSV) states. These setups are advantageous for long-distance detection and penetration through fog, clouds, or obstacles due to the longer wavelengths of microwaves. They also benefit from the ability to maintain coherence over larger distances. However, microwave systems require cryogenic cooling to achieve superconductivity, leading to larger, more complex, and costlier setups. Additionally, they face challenges with higher thermal noise compared to the optical domain, necessitating sophisticated noise suppression techniques.

In summary, optical quantum radar offers higher resolution and compactness but suffers from environmental limitations, while microwave quantum radar provides robustness and better long-distance performance but requires significant infrastructure and faces thermal noise challenges.

6. Limits of Quantum Radar

An analysis made on quantum illumination (QI) has been compared with a coherent classical illumination [1-3, 34]. As a result, the error probability upper bound (UB) and lower bound (LB) of the signals are determined as Eq. (14) and illustrated as in Fig. 4. In both Eq. (14) and Fig. 4, M is time-bandwidth product, N_S and N_I are the number of signal and idler photons, respectively and η is the reflection coefficient of the target [2].

$$\Pr(e)_{CI} \leq e^{-M\eta N_S/4N_B}/2 \quad (14.a)$$

$$\Pr(e)_{QI} \leq e^{-M\eta N_S/N_B}/2 \quad (14.b)$$

$$\Pr(e)_{CI} \leq e^{-M\eta N_S/2N_B}/4 \quad (14.c)$$

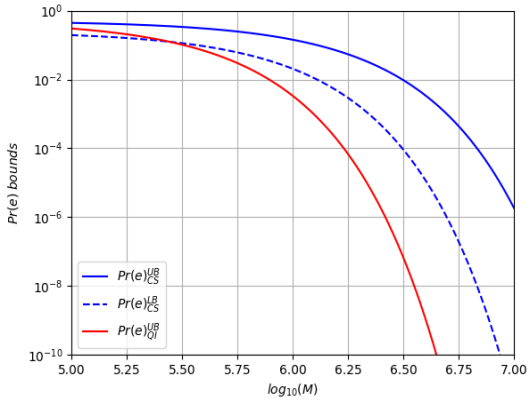

Fig. 4 Performance of QI compared to CI [2]

7. Practical Applications of Quantum Radar

Table 1 provides an overview of foundational research papers that have employed quantum illumination sources for quantum radar experiments across both the optical and microwave domains. The table is organized into four columns: the first column references the specific paper, the second column records the year of publication, tracing the evolution and growing interest in quantum radar technologies. The third column specifies the domain of the study, either optics or microwave. The final column lists the range between the transmitter and object, if specified, providing insight into the practical distance limitations and capabilities demonstrated in each experiment.

Table 1 Range analysis

Paper	Year	Domain	Range
[4]	2013	Optics	Not Specified
[6]	2015	Optics	Not Specified
[8]	2019	Optics	0.32 m
[9]	2019	Optics	0.19 m
[7]	2020	Optics	3 m
[16]	2020	Microwave	0.5 m
[19]	2020	Microwave	1 m
[25]	2022	Microwave	Not Specified

8. An Analysis on Quantum Radar Studies

In addition to the achievements of the quantum radar compared to the classical counterpart, studies on the quantum radar have been analyzed depending on the data from Google Scholar. The analysis of studies examines the development of academic publications in the fields of both quantum radar and quantum illumination in terms of authors and papers from 2008 to 2024. Since the first paper from Seth Lloyd is thought of as a seed for the quantum illumination story [1], analysis of studies started from 2008.
The first analysis is the number of papers and its annual variation from 2008 to 2024 as illustrated in Fig. 5. It's observed in Fig. 5, the interest is properly increasing on quantum radar about to 2020, then from 2020 to today even its not abruptly decrease, it shows lowering trends.

In addition to bar chart analysis, it is also provided that the mapping of the publications on the world map in 2024 in Fig. 6. Our analysis of geographical distribution indicates a concentration of research activities in specific regions. The United States, China, and various European countries are leading in contributions to quantum radar studies. The significant input from these regions can be attributed to their advanced technological and academic infrastructure. Moreover, since we cannot show the annual change of the papers that we visualized on the world map on a printout, we made it accessible on the web page that we provided as a reference in [58].

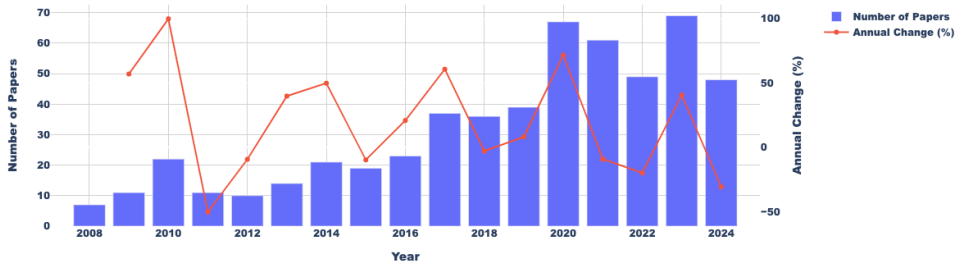

Fig. 5 The yearly variation of the papers written on quantum radar

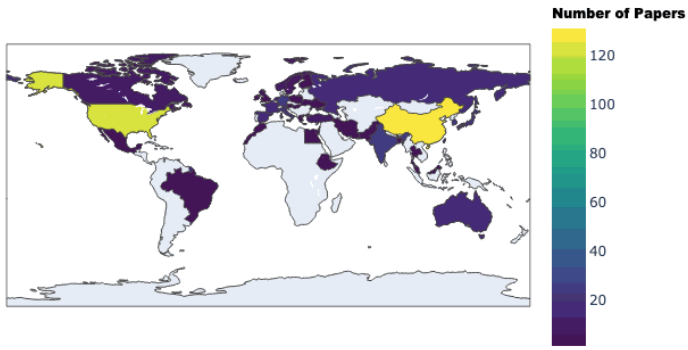

Fig. 6 Number of papers about quantum radar on world map in 2024.

Since we cannot show the annual change of the authors who are studying on quantum radar, that we visualized on the world map on a printout, we made it accessible on the web page that we provided as a reference in [59], it is illustrated in Fig. 7 for 2024. This analysis demonstrates that quantum radar research is gaining momentum with an increasingly diverse group of researchers engaging in the field. The global interest highlights the promising future of quantum radar technology, establishing it as an important area of study in the scientific domain.

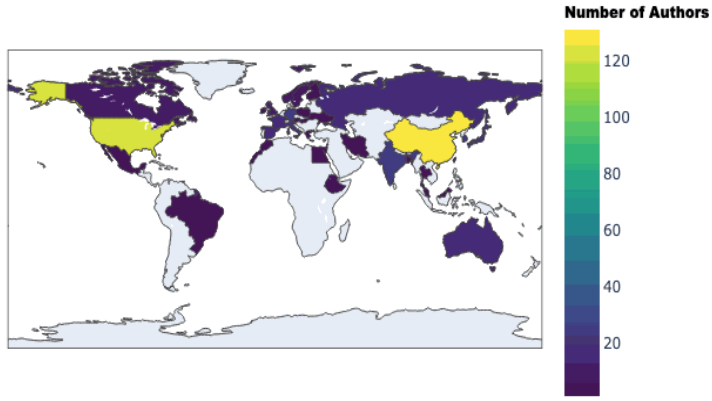

Fig. 7 Number of researchers studying on quantum radar on world map in 2024

When we look at the quantum radar studies in Türkiye, ASELSAN KUANTAL (Quantum Technologies Research Laboratory) is a cutting-edge research facility established to advance Türkiye's expertise in quantum technologies, focusing on applications for defense, sensor development, and secure communication systems [60]. Located at the TOBB University of Economics and Technology, KUANTAL is one of Türkiye's few dedicated quantum technology laboratories and is designed to drive high-impact research and innovation in areas like quantum radar, quantum cryptography, and quantum random number generation. Through collaborations with local and international research institutions, the laboratory aims to contribute to the development of advanced systems that leverage quantum properties, such as entanglement, for improved performance in detecting stealth targets, encrypted communications, and noise-resilient sensing.

9. Conclusion

In conclusion, this paper provides a comprehensive overview of the theoretical framework and experimental advancements in quantum radar, focusing on the generation and utilization of entangled signals. We have examined the methods used to produce quantum-correlated signals in both the optical and microwave domains, highlighting the distinct mechanisms and challenges associated with each. Following the generation of these signals, we discussed the measurement techniques employed to capture quantum information within optical and frequency domains. Theoretical limits on the performance of quantum radar were then explored, illustrating the potential and boundaries of these systems in terms of range, accuracy, and robustness against noise. By providing a table, we contextualized these findings within experimental setups across a range of conditions.

Finally, our analysis concludes with a broader examination of the field of quantum radar research, represented through a bar chart that aggregates study counts and a world map visualizing global research activity. The map illustrates the distribution of both published papers and contributing authors, underscoring the growing international interest driving the advancement of quantum radar technologies. This overview not only highlights the progress made in the field but also identifies areas for further exploration, particularly in experimental implementations and practical applications, as the global scientific community continues to advance this promising area of quantum technology.

References

1. Loyd S. Enhanced sensitivity of photodetection via quantum illumination. Science, 2008; 321(6895): 1463 – 1465.
2. Tan S H, Erkmen B I, Giovannetti V, Guha S, Lloyd S, Maccone L, Pirandola S, and Shapiro J H. Quantum illumination with Gaussian states. Physical Review Letter, 2008;105(25): 243601.
3. Shapiro J H, and Lloyd S. Quantum illumination versus coherent-state target detection. New Journal of Physics, 2009;11(6): 053045.
4. Lopaeva E D, Ruo Berchera I, Degiovanni I P, Olivares S, Brida G, and Genovese M. Experimental realization of quantum illumination. Physical Review Letter, 2013;110(15): 156603.
5. Zhao J, Lyons A, Ulku A C, Defienne H, Faccio D, and Charbon E. Light detection and ranging with entangled photons. Optics Express, 2022;30(3): 3675 – 3683.
6. Zhang Z, Mouradian S, Wong F N C, and Shapiro J H. Entanglement-enhanced sensing in a lossy and noisy environment. Physical Review Letter, 2015;114(11): 110506.
7. Frick S, McMillan A, and Rarity J. Quantum rangefinding. Optics Express, 2020;28(25): 37118 – 37128.

8. England D G, Balaji B, and Sussman, B J. Quantum-enhanced standoff detection using correlated photon pairs. Physical Review Letter, 2019;99(2): 023828.
9. Liu H, Giovannini D, He H, England D, Sussman B J, Balaji B, and Helmy A S. Enhancing LIDAR performance metrics using continuous-wave photon-pair sources. Optica, 2019;6(10): 1349 – 1355.
10. He H, Giovannini D, Liu H, Chen E, Yan Z, and Helmy A S. Non-classical semiconductor photon sources enhancing the performance of classical target detection systems. Journal of Lightwave Technology, 2020;38(16): 4540 – 4547.
11. Liu H, Balaji B, and Helmy A S. Target detection aided by quantum temporal correlations: theoretical analysis and experimental validation. IEEE Transactions on Aerospace and Electronic Systems, 2020;56(5): 3529 – 3544.
12. Blakey P S, Liu H, Papangelakis G, Zhang Y, Léger Z M, Iu M L, and Helmy A S. Quantum and non-local effects offer over 40 dB noise resilience advantage towards quantum lidar. Nature Communications, 2022;13(1): 5633.
13. Barzanjeh S, Guha S, Weedbrook C, Vitali D, Shapiro J H, and Pirandola S. Microwave quantum illumination. Physical Review Letter, 2015;114(8): 080503.
14. Chang C W S, Vadiraj A M, Bourassa J, Balaji B, and Wilson C M. Quantum-enhanced noise radar. Applied Physics Letter, 2019;114(11): 112601.
15. Luong D, and Balaji B. Quantum two-mode squeezing radar and noise radar: covariance matrices for signal processing. IET Radar, Sonar & Navigation, 2020;14(1): 97 - 104.
16. Luong D, Chang S W S, Vadiraj A M, Damini A, Wilson C M, and Balaji B. Receiver operating characteristics for a prototype quantum two-mode squeezing radar. IEEE Transactions on Aerospace and Electronic Systems, 2020;56(3): 2041 - 2060.
17. Luong D, Balaji B, and Rajan S. Quantum two-mode squeezing radar and noise radar: correlation coefficient and integration time. IEEE Access, 2020;8: 185544 – 185547.
18. Luong D, Rajan S, and Balaji B. Quantum two-mode squeezing radar and noise radar: correlation coefficients for target detection, IEEE Sensors Journal, 2020; 20(10): 5221 – 5228.
19. Barzanjeh S, Pirandola S, Vitali D, and Fink J M. Microwave quantum illumination using digital receiver. Science Advances, 2020;16(9): p.eabb0451.
20. Guha S, and Erkmen B I. Gaussian-state quantum-illumination receivers for target detection. Physical Review A, 2009;80(5): 052310.
21. Norouzi M, Seyed-Yazdi J, Hosseiny S M, and Livreri P. Investigation of the JPA-bandwidth improvement in the performance of the QTMS radar. Entropy, 2023;25(10): 1368.
22. Hosseiny S M, Norouzi M, Seyed-Yazdi J, and Irannezhad F. Purity in the QTMS radar. Physica Scripta, 2023;98(5): 055105.
23. Hosseiny S M, Norouzi M, Seyed-Yazdi J, and Irannezhad F. Performance improvement factors in quantum radar/illumination. Communication in Theoretical Physics, 2023;10(5): 055101.
24. Norouzi M, Hosseiny S M, Seyed-Yazdi J, and Irannezhad F, Observation of the performance enhancement of a non-degenerate JPA versus degenerate JPA in a QTMS radar simulation. Engineering Research Express, 2024;6(1): 015030.
25. Livreri P, Enrico E, Fasolo L, Greco A, Rettaroli A, Vitali D, Farina A, Marchetti C F, and Giacomin A Sq D. Microwave quantum radar using a Josephson traveling wave parametric amplifier. 2022 IEEE Radar Conference (RadarConf2022); 2022 Mar 21-25; New York City, NY, USA. p. 1-5.

26. Qiu J Y, Grimsmo A, Peng K et al. Broadband squeezed microwaves and amplification with a Josephson travelling-wave parametric amplifier. Nature Physics, 2023;19: 706 - 713.
27. Esposito M, Ranadive A, Planat L et al. Observation of two-mode squeezing in a traveling wave parametric amplifier. Physical Review Letter, 2022;128(15): 153603.
28. Livreri P, Enrico E, Vitali D, and Farina A. Microwave quantum radar using a Josephson traveling wave parametric amplifier and a phase-conjugate receiver for a long-distance detection. 2023 IEEE Radar Conference (RadarConf23); 2023 May 1-5; San Antonio, TX, USA. p. 1-5.
29. Wei R, Li J, Wang W, Ye Z, Zhao C, and Guo Q. Evaluating the detection range of microwave quantum illumination radar. IET Radar Sonar Navigation, 2023;17(11): 1664 - 1673.
30. Sisco B, and Chen K C. Quantum wireless imaging and remote sensing - state-of-the-art technologies and opportunities. 2023 26th International Symposium on Wireless Personal Multimedia Communications (WPMC); 2023 Nov 19-22; Tampa, FL, USA. p. 293 - 298.
31. Luong D, Balaji B, and Rajan S. Biomedical sensing using quantum radars based on Josephson parametric amplifiers. 2021 International Applied Computational Electromagnetics Society Symposium (ACES); 2021 Aug 1-5; Hamilton, ON, Canada. p. 1-4.
32. Pirandola S, Bardhan, B R, Gehring, T, Weedbrook C, and Lloyd S. Advances in photonic quantum sensing. Nature Photonics, 2018;12: 724 - 733.
33. Balaji B. Quantum radar: snake oil or good idea?. 2018 International Carnahan Conference on Security Technology (ICCST), 2018 Oct 22-25; Montreal, QC, Canada. p. 1-7.
34. Shapiro J H. The quantum illumination story. IEEE Aerospace and Electronic Systems Magazine, 2020;35(4): 8 - 20.
35. Slepyan G, Vlasenko S, Mogilevtsev D, and Boag A. Quantum radars and lidars: concepts, realizations, and perspectives. IEEE Antennas and Propagation Magazine, 2022;64(1): 16 - 26.
36. Torromé R G, and Barzanjeh. Advances in quantum radar and LIDAR. Progress in Quantum Electronics, 2023; 93: 100497.
37. Luong D, Balaji B, and Rajan S. Quantum radar: challenges and outlook: an overview of the state of the art. IEEE Microwave Magazine, 2023; 24(9): 61 - 67.
38. Karsa A, Fletcher A, Spedalieri G, and Pirandola S. Quantum illumination and quantum radar: a brief overview. Reports on Progress in Physics, 2024; 87(9): 094001.
39. Lin Y -C, Huang T -W, Tsai P -J, Chen Y -H, Zhong Y -L, and Chang C -R. Advancements in quantum radar technology an overview of experimental methods and quantum electrodynamics considerations. IEEE Nanotechnology Magazine, 2024;18(3): 4 - 14.
40. Walls D F, and G. J. Milburn, Quantum Optics, 2nd edition. Berlin:Springer-Verlag Berlin Heidelberg; 2008.
41. Caves C M, and Schumaker B L. New formalism for two-photon quantum optics. I. Quadrature phases and squeezed states. Physical Review A, 1985;31(5): 3068 - 3092.
42. Schumaker B L, and Caves C M. New formalism for two-photon quantum optics. II. Mathematical foundation and compact notation. Physical Review A, 1985;31(5): 3093 - 3111.
43. Lecture Notes: From Nonlinear Optics to Entanglement and Squeezing. [Document on the Internet]; [cited 2024 October 18]. Available from:

https://mpl.mpg.de/research-at-mpl/independependent-research-groups/chekhova-research-group/teaching.
44. Fox M. Quantum optics: an introduction. New York:Oxford University Press; 2006.
45. Ghambaryan I A, Guoa R, Hovsepyan R K, Poghosyan A R, Vardanyan E S, and Lazaryan V G. Periodically poled structures in lithium niobate crystals: growth and photoelectric properties. Journal of Optoelectronics and Advanced Materials, 2003; 5(1): 61 - 68.
46. Lithium Niobate, [cited 2024 December 05]. Available from: https://www.tydexoptics.com/pdf/Lithium_Niobate.pdf
47. Lithium Niobate, [cited 2024 December 05]. Available from: https://roditi.com/SingleCrystal/LiNbO3/Magnesium-Doped.html
48. Hum D S, and Fejer M M. Quasi-phasematching. Comptes Rendus - Physique, 2007; 8(2): 180 - 198.
49. Tambasco J-L, Boes A, Helt L G, Steel M J, and Mitchell A. Domain engineering algorithm for practical and effective photon sources, 2016; Optics Express, 24(17): 19616 - 19626.
50. Smith B J, Mahou P, Cohen O, Lundeen J S, and Walmsley I A. Photon pair generation in birefringent optical fibers, 2009; Optics Express 17(26): 23589 - 23602.
51. Orieux A, Versteegh M A M, Jöns K D, and Ducci S. Semiconductor devices for entangled photon pair generation: a review, 2017; Reports on Progress in Physics, 80(7): 076001.
52. Caves C M, and Schumaker B L. New formalism for two-photon quantum optics. I. Quadrature phases and squeezed states, 1985; Physical Review A, 31(5): 3068 - 3092.
53. Schumaker B L, and Caves C M. New formalism for two-photon quantum optics. II. Mathematical foundation and compact notation, 1985; Physical Review A, 31(5): 3093 - 3111.
54. Braunstein S L, and van Loock P. Quantum information with continuous variables, 2005; Review of Modern Physics, 77(2): 513 - 577.
55. Weedbrook C, Pirandola S, and García-Patrón R, Cerf N J, Ralph T C, and Shapiro J H, and Lloyd S. Gaussian quantum information, 2012; Review of Modern Physics, 84(2): 621 -669.
56. Abdo B, Kamal A, and Devoret M. Nondegenerate three-wave mixing with the Josephson ring modulator, 2013; Physical Review B, 87(1): 014508.
57. Ulku A C, Bruschini C, Antolović I M, Kuo Y, Ankri R, Weiss S, Michalet X, and Charbon E. A 512 × 512 SPAD image sensor with integrated gating for widefield FLIM. IEEE Journal of Selected Topics in Quantum Electronics, 2019; 25(1): 1 - 12.
58. Number of Papers on Quantum Radar. [cited 2024 October 25]. Available from: https://krccorp.net/papers.gif.
59. Number of Authors working on Quantum Radar. [cited 2024 October 25]. Available from: https://krccorp.net/authors.gif.
60. ASELSAN QUANTAL. [Document on the Internet]; [cited 2024 October 25]. Available from: https://www.aselsan.com/en/research-and-development/quantum-technologies.